

# Dental Materials

## Finite element analysis of narrow dental implants

--Manuscript Draft--

<b>Manuscript Number:</b>	DENTMA-D-19-00040R1
<b>Article Type:</b>	Full Length Article
<b>Keywords:</b>	Osseointegration; Dental Implantation, Endosseous; Maxilla; Jaw, Edentulous; Stress, Mechanical; compressive strength; tensile strength; Dental Prosthesis, implant-supported; Dental Implant, single tooth; Dental implant
<b>Corresponding Author:</b>	Eduard Valmaseda-Castellon, DDS, MS, PhD University of Barcelona L'Hospitalet de Llobregat, Barcelona SPAIN
<b>First Author:</b>	José Fernando Valera-Jiménez
<b>Order of Authors:</b>	José Fernando Valera-Jiménez
	Genís Burgueño-Barris, DDS
	Sergio Gómez-González
	Josep López-López
	Eduard Valmaseda-Castellon, DDS, MS, PhD
	Enrique Fernández-Aguado
<b>Abstract:</b>	<p>Narrow-diameter implants (NDIs) traditionally have been associated to higher rates of failure in comparison with regular-diameter implants (RDIs) and wide-diameter implants (WDIs), since they generate a more unfavorable stress distribution in peri-implant bone. However, it is well known that the load sharing effect associated with prostheses supported by multiple implants (also called splinted prostheses) affords mechanical benefits. The present study involves finite element analysis (FEA) to determine whether the risks linked to NDIs could be mitigated by the mechanical advantages afforded by the splinting concept. For this purpose, a three-dimensional (3D) model of a real maxilla was reconstructed from computed tomography (CT) images, and different implants (NDIs, RDIs and WDIs) and prostheses were created using computer-aided design (CAD) tools. Biting forces were simulated on the prostheses corresponding to three different rehabilitation solutions: single-implant restoration, three-unit bridge and all-on-four treatment. Stress distribution around the implants was calculated, and overloading in bone was quantified within peri-implant volumes enclosed by cylinders with a diameter 0.1 mm greater than that of each implant. The mechanical benefits of the splinting concept were confirmed: the peri-implant overload volume around NDIs splinted by means of the three-unit bridge was significantly reduced in comparison with the non splinted condition and, most importantly, proved even smaller than that around non splinted implants with a larger diameter (RDIs). However, splinted NDIs supporting the all-on-four prosthesis led to the highest risk of overloading found in the study, due to the increase in compressive stress generated around the tilted implant when loading the cantilevered molar.</p>
<b>Response to Reviewers:</b>	

Barcelona, July the 25<sup>th</sup> 2019

Dear Dr. Watts,

We submit the manuscript entitled "FINITE ELEMENT ANALYSIS OF NARROW DENTAL IMPLANTS" for your consideration to be published in the Dental Materials Journal.

The article is original, it has not been submitted elsewhere, and it is free of conflicts of interest. It addresses stress distribution in narrow diameter implants connected to single tooth prosthesis, partial fixed bridges and a full arch prosthesis. We would like to have figures 2, 3 and 4 printed in color.

All the signing authors have read and approved the final version of the manuscript and comply with the requirements for authorship. Furthermore, the authors state that the data presented in this manuscript are real and accurate.

We suggest as reviewers:

Frank Schwarz. Department of Oral Surgery. Universitätsklinikum Düsseldorf. Düsseldorf. Germany. Email: F.Schwarz@med.uni-frankfurt.de

Dohyung Lim. Department of Mechanical Engineering, Sejong University, Seoul 05006, Korea. Email: dli349@sejong.ac.kr

Angel Insua Brandariz, Facultad de Medicina y Odontología, C/Entrerrios s/n., Santiago de Compostela., A Coruña., España, Phone: +34 881 81 22 19, Fax: +34981582642, email: ainsua@umich.edu

Yours sincerely,

Eduard Valmaseda-Castellón on behalf of the rest of the authors.

Dear Dr. Watts,

We resubmit the manuscript entitled "FINITE ELEMENT ANALYSIS OF NARROW DENTAL IMPLANTS" (DENTA-19-00040) after addressing your request of a major revision. We have addressed all the comments of the reviewers, which helped us to improve the manuscript. Below you will find our answers to the comments. All changes are highlighted in yellow in the final manuscript. Figures 3 and 4 have been modified as well to comply with comment 7.

**Comment 1:** *Results. The authors described that "The reason for distinguishing between minimum and maximum principal stress is to see the difference between compressive and tensile stress patterns respectively." However, the positive values of maximum/minimum principal stress mean tensile stress. The negative values of maximum/minimum principal stress mean compressive stress. Revise all related points.*

**Answer 1:** We thank you for your constructive recommendations to improve the quality of our work. Indeed, the sentence was not strictly correct since it is true that positive values of principal stress mean tension and negative ones mean compression. In the new version of the manuscript we have solved this ambiguity with a more precise sentence: *"The reason for distinguishing between minimum and maximum principal stress is to identify the areas where overloading occurs due to either compressive or tensile stress, respectively, according to the maximum normal stress criterion defined above"*. In fact, based on this stress criterion used for brittle materials, overloading of bone occurs when the maximum principal stress exceeds its tensile strength or when the minimum principal stress exceeds its compressive strength.

**Comment 2:** *Discussion. References in the Discussion section is not enough. Ex. The last sentence in the first paragraph should be referred similar studies.*

**Answer 2:** Thanks for this observation. In the new manuscript, we have included more references supporting our discussion.

**Comment 3:** *Some results such as " $\langle OV \rangle_{3.0mm} = 2.20 \text{ mm}^3$ " were described in the Discussion section. These results must be moved to the Results section. Make sure and revise all related points.*

**Answer 3:** We included those data in the Discussion section since they give rise to a particular analysis from the general data provided in the Figure 3 (Results section). In any case, it is true they fit better in the Results section. We have moved this and other numerical data to the Results section while keeping their interpretation in the Discussion section.

**Comment 4:** *Also, what's the meaning of OV? Define it.*

**Answer 4:** Overloading is a major trigger for the damage and resorption of peri-implant bone. OV means overloaded volume and is related to the stress criterion we have considered to determine the areas under overloading in bone, in accordance with similar studies. It should be noted that bone can be damaged by tensile or compressive stress.

According to the maximum principal stress theory, as two possible circumstances in which materials can be damaged, tensile overloading occurs when the maximum principal stress exceeds the tensile strength of the material and compressive overloading occurs when the minimum principal stress exceeds the compressive strength of the material. OV represents the volume of the regions where the stress exceeds the bone strength (under both tension and compression). That is why we have calculated  $OV_T$  (overloaded volume under tension) and  $OV_C$  (overloaded volume under compression), OV being the sum of both terms.

We would like to thank your comment since it has made us realize that our explanation was not clear enough in the text. In the new version of the manuscript, we have made an effort to define it better:

*“Therefore, in the present paper the overloading risk in bone for the different prosthetic solutions was measured through the quantification of the partial volume overloaded under tension ( $OV_T$ ), where the maximum principal stress exceeds the tensile strength of bone, and the partial volume overloaded under compression ( $OV_C$ ), where the minimum principal stress exceeds the compressive strength of bone, with the total overloaded volume (OV) being the sum of both contributions:  $OV = OV_T + OV_C$ .”*

**Comment 5:** Future works were described in the Conclusion section. They must be moved to the Discussion section.

**Answer 5:** Thanks for this observation. This has been solved in the new version of the manuscript.

**Comment 6:** The reference numbers should be located before the period. Revise all related points.

**Answer 6:** This inconvenience has been corrected in the new manuscript.

**Comment 7:** The period should be used for all decimal points. Ex. "2,04 mm<sup>3</sup>" should be modified to "2.04 mm<sup>3</sup>".

**Answer 7:** Sorry for this issue. Both the text and the figures (3 and 4) have been modified.

Besides this changes, we have also changed the terms “non-splinted” and “non-splinted” to “nonsplinted”. However, if any of the former 2 terms is preferred to comply with journal style, it might be changed accordingly.

Yours sincerely,

**Title:** Finite element analysis of narrow dental implants.

**Authors names:** Valera-Jiménez J.F.<sup>a,b</sup>, Burgueño-Barris G.<sup>c</sup>, Gómez-González S.<sup>a</sup>,  
López-López J.<sup>a</sup>, Valmaseda-Castellón E.<sup>d</sup> and Fernández-Aguado E.<sup>a</sup>

**Affiliations:**

<sup>a</sup>Research Group of Interacting Surfaces in Bioengineering and Materials Science (InSup), Department of Materials Science and Metallurgical Engineering, Technical University of Catalonia (UPC), Avda. Diagonal 647, 08028-Barcelona, Spain.

<sup>b</sup>At present: Laboratorio de Impresión 3D y Pilas de Combustible (3D-ENERMAT), Instituto de Energías Renovables, University of Castilla La Mancha, P. Investigación 1, 02071-Albacete, Spain.

<sup>c</sup>DDS, Master of Oral Surgery and Implantology. Associate professor of the Master degree program in Oral Surgery and Implantology, Faculty of Dentistry, University of Barcelona. Barcelona, Spain.

<sup>d</sup>DDS, MS, PhD. Master of Oral Surgery and Implantology. Professor of Oral Surgery. Director of the Master degree program in Oral Surgery and Implantology, Faculty of Dentistry, University of Barcelona. Researcher at the IDIBELL institute. Barcelona, Spain.

**Corresponding author:**

Eduard Valmaseda-Castellón

Facultat de Medicina i Ciències de la Salut. Campus de Bellvitge. C/Feixa llarga s/n.  
L'Hospitalet de Llobregat 08907. Barcelona. Spain. Phone: +34618276129. Email:  
eduardvalmaseda@ub.edu

## ABSTRACT

Narrow-diameter implants (NDIs) traditionally have been associated to higher rates of failure in comparison with regular-diameter implants (RDIs) and wide-diameter implants (WDIs), since they generate a more unfavorable stress distribution in peri-implant bone. However, it is well known that the load sharing effect associated with prostheses supported by multiple implants (also called splinted prostheses) affords mechanical benefits. The present study involves finite element analysis (FEA) to determine whether the risks linked to NDIs could be mitigated by the mechanical advantages afforded by the splinting concept. For this purpose, a three-dimensional (3D) model of a real maxilla was reconstructed from computed tomography (CT) images, and different implants (NDIs, RDIs and WDIs) and prostheses were created using computer-aided design (CAD) tools. Biting forces were simulated on the prostheses corresponding to three different rehabilitation solutions: single-implant restoration, three-unit bridge and all-on-four treatment. Stress distribution around the implants was calculated, and overloading in bone was quantified within peri-implant volumes enclosed by cylinders with a diameter 0.1 mm greater than that of each implant. The mechanical benefits of the splinting concept were confirmed: the peri-implant overloaded volume around NDIs splinted by means of the three-unit bridge was significantly reduced in comparison with the nonsplinted condition and, most importantly, proved even smaller than that around nonsplinted implants with a larger diameter (RDIs). However, splinted NDIs supporting the all-on-four prosthesis led to the highest risk of overloading found in the study, due to the increase in compressive stress generated around the tilted implant when loading the cantilevered molar.

## **ACKNOWLEDGMENTS**

The authors thank public funding received through the projects DPI2016-77768-R (Ministerio de Economía y Competitividad, Spain) and 2017SGR253 (Agència de Gestió d'Ajuts Universitaris i de Recerca, Generalitat de Catalunya, Spain).

**KEYWORDS:** Osseointegration; Dental Implantation, Endosseous; Maxilla; Jaw, Edentulous; Stress, Mechanical; Compressive Strength; Tensile Strength; Dental Prosthesis, implant-supported; Dental Implant, single tooth; Dental Implant,

## INTRODUCTION

In recent years, dental implants have been used as surgical components in a wide variety of oral restoration scenarios, including single-tooth replacements or multiple implant-supported bridgeworks replacing various missing teeth. The success of the treatment depends on a number of biological and mechanical factors. Even when implants are fully osseointegrated, there is a risk of bone resorption in the peri-implant regions, which can be activated by bacterial infection or overloading due to masticatory forces [1]. Overloading is often the result of inefficient stress distribution generated by inappropriate occlusion, implant design or positioning. In this context, an increased area of bone-to-implant contact (BIC) may reduce the risk of overloading in peri-implant bone by improving osseointegration and achieving a more balanced stress distribution. Among the options in pursuit of this objective, increasing the implant diameter has proven to be a successful strategy [2-4].

The term narrow-diameter implants (NDIs) usually refers to implants with a diameter < 3.4 mm [5]. Such diameters are reportedly large enough to provide satisfactory long-term outcomes. In some clinical situations, NDIs represent an option for restoring narrow alveolar ridges and sites with limited space for the insertion of standard diameter implants (SDIs), reducing the need for bone augmentation procedures [5,6]. Although some follow-up studies have reported similar survival rates for NDIs and SDIs [7,8], it has been stated that the resistance of NDIs is 25% less than that of SDIs [9], and that the risk of fatigue fracture increases when using small diameters [10]. Furthermore, some studies based on finite element analysis (FEA) have concluded that narrow diameters involve higher stress and strain levels at peri-implant bone level when compared with



conventional diameters, anticipating a higher rate of bone loss [11,12]. These concerns explain the fact that NDIs traditionally have been restricted to concrete situations such as the rehabilitation of incisors but are not commonly used in areas exposed to high masticatory forces such as the molar regions [6].

On the other hand, the term splinting (or stabilization) refers to binding teeth or implants together to increase the stability of the structure as a whole. The rationale behind splinted implant prostheses is to achieve favorable distribution of non-axial forces and increase the total area receiving the load. Some authors have reported that splinting implies biomechanical advantages and leads to load sharing [13]. However, research on the clinical use of splinted NDIs is still limited [5]. Similarly, FEA studies are generally focused on single-unit restorations or fixed prostheses supported by multiple SDIs, but FEA-based studies evaluating multiple NDI-supported prostheses are still scarce. Although splinted mini-implants (1.8 mm in diameter) compared with single mini-implants clinically show a similar bone loss [14], splinting of implants reduces the tensile stress in the posterior area of short fixed bridges [15]. Accordingly, the present study used FEA to determine whether the risks associated with NDIs could be decreased to a significant degree by the load-sharing effect resulting from the splinting concept.

## **MATERIALS AND METHODS**

In this study, the biomechanical benefits associated with splinted NDIs were investigated by FEA. In order to allow quantitative comparisons between different implant diameters, the study was extended to regular-diameter implants (RDIs) and wide-diameter implants (WDIs). Three prosthetic solutions including nonsplinted and splinted implants were

three-dimensionally (3D) modeled as shown in Figure 1. Firstly, the InVesalius 3.0 software (<http://www.cti.gov.br/invesalius/>) was used to reconstruct a maxilla from DICOM images of an upper jaw belonging to a 72-year-old edentulous male. The reconstructed maxilla was imported to Solidworks® (Dassault Systèmes Solid Works® Corp., Concord, USA), and two different regions were generated: an inner volume simulating cancellous bone and an external layer representing cortical bone. The thickness of the cortical layer in the different regions of the maxilla was selected in accordance with other authors [16]. Two different maxillary bone segments were generated: one half of the maxilla without the sinuses (for single-implant restorations and three-unit bridges) and a “full” maxilla conserving the maxillary sinuses (for all-on-four treatments).

Three-dimensional implants and superstructures were designed via CAD with Solidworks® and 3D modelling software. The implants were based on commercially available components (ADIN® Dental Implant Systems, Ltd., Afula, IL, USA). A total of 6 implants were created: implants with three different diameters (NDI - 3.0 mm; RDI - 3.5 mm; and WDI - 4.3 mm) of two different lengths (10 mm and 13 mm). Straight and 30°-angled abutments based on the same brand were also generated. On the other hand, three single dental structures (supported by individual implants) and a splinted three-unit bridge (supported by two implants) replacing the first premolar, second premolar and first molar were modeled. A splinted full arc bridge, characteristic of the all-on-four concept [17], was also designed. In the case of the single-implant rehabilitation and the three-unit bridge, 10 mm long implants and straight abutments with a transmucosal height of 3 mm were used. For the all-on-four concept, posterior 13 mm long implants were attached to angled abutments with a transmucosal height of 3 mm, and anterior 10 mm long implants

were connected to straight abutments with a transmucosal height of 2 mm. On the basis of other studies [11], cratering effects were modeled around the abutment to simulate the well-known bone resorption that occurs in the areas close to the implant neck.

The models were transferred from Solidworks® to COMSOL Multiphysics® (COMSOL, Inc., Burlington, USA) to carry out static linear elastic simulations. The material properties assigned to each domain are given in Table 1 [18-21]. A zero-displacement boundary condition was defined for the flat faces of the maxillary segments. Three different loading scenarios were considered for each of the three rehabilitation solutions: first premolar loaded (250 N), second premolar loaded (300 N) and first molar loaded (300 N). The loads were uniformly distributed in the occlusal regions, and their magnitudes were similar to experimental single tooth bite forces in healthy young male adults [22]. The angle between the implants axes and the forces was 15° [23]. The direction of the force vector was based on the maximum forces analyzed in previous studies [24]. Total osseointegration of the implants was considered, since node-to-node correspondences at the interface between the implants and bone were assumed. After a convergence test, the models representing the single-implant restoration, the three-unit bridge and the all-on-four rehabilitation were meshed with approximately 0.7, 1.2 and 3 million elements, respectively. Finally, the solutions were computed and the data of specific volumes of interest (VOIs) were extracted for quantitative evaluation of the results. Such volumes (shown in Figure 1) included the fraction of peri-implant cancellous and cortical bone enclosed by cylinders of different diameters (3.1 mm, 3.6 mm and 4.4 mm), depending on the implant diameter (3.0 mm, 3.5 mm and 4.3 mm, respectively).

In accordance with similar studies [11, 25], overloading of cancellous and cortical bone was considered to occur when the maximum or minimum principal stresses exceeded their uniaxial tensile or compressive strength, respectively. This consideration was made on the basis of the maximum normal stress criterion, usually linked to brittle materials. The strength of cortical bone was assumed to be 100 MPa under tension and 170 MPa under compression. In cancellous bone, a strength of 5 MPa was adopted for both tension and compression [26]. Therefore, in the present paper the overloading risk in bone for the different prosthetic solutions was measured through the quantification of the partial volume overloaded under tension ( $-OV_T$ ), where the maximum principal stress exceeds the tensile strength of bone, and the partial volume overloaded under compression ( $OV_C$ ), where the minimum principal stress exceeds the compressive strength of bone, with the total overloaded volume (OV) being the sum of both contributions:  $OV = OV_T + OV_C$ .

## RESULTS

Figure 2 shows, as a comparative example of the stress field around splinted and nonsplinted implants, the distribution of maximum and minimum principal stress in the models corresponding to the single-implant rehabilitation and the three-unit bridge, specifically when loading the first premolar. The reason for distinguishing between minimum and maximum principal stress is to identify the areas where overloading occurs due to either compressive or tensile stress, respectively, according to the maximum normal stress criterion defined above. The cross sections in this figure were obtained by selecting planes containing the direction of the force applied.

Figure 2 offers a comprehensive view of the effect of the implant diameter on the stress distribution in bone. A decrease in size of the areas affected by stress levels above or close to the physiological limits occurs when the implant diameter is increased. Furthermore, on comparing the single-implant rehabilitation with the two-implant-supported bridge, a reduction in stress levels around the first premolar (P1; where the load is applied) is noticed. This is obviously a result of the splinting concept and its subsequent load-sharing effect. Such observations can be verified in quantitative terms in Figure 3, which depicts the mean principal maximum and minimum stress in the VOIs around the implants supporting the single restoration and the bridge, together with the magnitude of the total overloaded volume within these VOIs (i.e. OV). It should be remembered that OV encompasses both the partial overloaded volume under tension (OV<sub>T</sub>; i.e. those regions in which the maximum principal stress exceeds the uniaxial tensile strength of bone) and the partial overloaded volume under compression (OV<sub>C</sub>; i.e. those regions where the minimum principal stress exceeds the uniaxial compressive strength of bone).

Focusing on the nonsplinted restorations as the simplest example to assess the effect of the implant diameter on the overloading risk, if the data in Figure 3 corresponding to the total overloaded volumes around the single implants for the three loading conditions (i.e. P1, P2 and M1 loaded) is averaged, the values obtained are the following:  $\langle OV \rangle_{3.0\text{ mm}} = 2.20\text{ mm}^3$ ,  $\langle OV \rangle_{3.5\text{ mm}} = 1.62\text{ mm}^3$  and  $\langle OV \rangle_{4.3\text{ mm}} = 0.93\text{ mm}^3$  in cancellous bone; and  $\langle OV \rangle_{3.0\text{ mm}} = 0.04\text{ mm}^3$ ,  $\langle OV \rangle_{3.5\text{ mm}} = 0.02\text{ mm}^3$  and  $\langle OV \rangle_{4.3\text{ mm}} = 0.01\text{ mm}^3$  in cortical bone. As illustrated in Figure 1, the amount of cortical bone in the VOIs analyzed is significantly less than that of cancellous bone, which explains the difference in the magnitude of the overloaded volume in both tissues. Thus, the average overloaded volumes shown above indicate that the overloading risks in the peri-implant areas are

reduced when increasing the implant diameter, this trend being observed in each loading condition.

Similarly, Figure 3 also provides information about the mechanical advantages of the splinting concept. To facilitate comparisons, hereinafter the terms  $OV_{NS}$  and  $OV_S$  will be used to denote the overloaded volume around nonsplinted implants (single implants) and the overloaded volume around splinted implants (those supporting the 3-unit bridge), respectively. For example, for the 3 mm diameter implant P1 under direct loading (that is, when the load is applied on the tooth supported by such implant), a reduction from  $OV_{NS-3.0\text{ mm}} = 2.04\text{ mm}^3$  to  $OV_{S-3.0\text{ mm}} = 1.20\text{ mm}^3$  is found in cancellous bone. In cortical bone, this value decreases from  $OV_{NS-3.0\text{ mm}} = 0.04\text{ mm}^3$  to  $OV_{S-3.0\text{ mm}} = 0.01\text{ mm}^3$ . An interesting approach to quantify such reductions could be to introduce the consideration of a nonsplinted implant of larger diameter in the analysis. When looking at the nonsplinted 3.5 mm diameter implant P1, the total overloaded peri-implant volume is  $OV_{NS-3.5\text{ mm}} = 1.52\text{ mm}^3$  in cancellous bone and  $OV_{NS-3.5\text{ mm}} = 0.02\text{ mm}^3$  in cortical bone. The interest in this assessment lies in the fact that the overloaded peri-implant volume for the splinted 3.0 mm diameter implant P1 is smaller than that around a larger diameter nonsplinted implant located in the same position, even when higher overloading should be expected for the smaller-diameter implant. The mean stress around splinted  $P1_{3.0\text{ mm}}$  is also below that around nonsplinted  $P1_{3.5\text{ mm}}$ .

The same is true when the analysis is done for the implant M1 under direct loading: the values of overloaded volume are  $OV_{NS-3.0\text{ mm}} = 2.98\text{ mm}^3$ ,  $OV_{S-3.0\text{ mm}} = 1.40\text{ mm}^3$  and  $OV_{NS-3.5\text{ mm}} = 2.34\text{ mm}^3$  in cancellous bone, and  $OV_{NS-3.0\text{ mm}} = 0.06\text{ mm}^3$ ,  $OV_{S-3.0\text{ mm}} = 0.01\text{ mm}^3$  and  $OV_{NS-3.5\text{ mm}} = 0.03\text{ mm}^3$  in cortical bone. However, in

both cases, the stress levels and the regions affected by overloading around nonsplinted 4.3 mm diameter implants remain below those surrounding splinted 3.0 mm diameter implants.

Finally, Figure 4 shows the results of the simulations regarding the all-on-four splinted prosthesis. As seen in the figure, the mechanical behavior of the all-on-four restoration varies considerably depending on the loading condition involved. When loading the first premolar, the scenario is favorable in mechanical terms. However, if the arch is loaded on the first molar, the peri-implant VOI of cancellous bone around the tilted implant P2<sub>L</sub> experiences the highest magnitude of overloaded volume found in the study (for example,  $OV = 3.43 \text{ mm}^3$  when considering 3 mm diameter implants), even higher than the values around the single-implant restorations. Although not shown in Figure 4 for simplicity, the mean minimum principal stress around P2<sub>L</sub> was also significant in this case (for example,  $\langle \sigma_{p \min} \rangle = -1.98 \text{ MPa}$  for the 3 mm diameter implants).

## DISCUSSION

Quantitatively, an accurate translation of the findings of this study to the clinical setting should not be expected, since they are part of a numerical method that has introduced several simplifications. Among these limitations, a condition of 100% osseointegration was assumed, cancellous and cortical bone were regarded as isotropic linearly elastic materials, and the loads selected were static and not time-dependent. However, similar studies based on stress analysis using FEA have yielded an approximate idea of the stress distribution and overloading risk in peri-implant tissues [11,12,27-30], and have been helpful in the anticipation of mechanical testing and clinical results [31-32].

The effect of the implant diameter on the stress distribution around the peri-implant regions was the same observed by other authors [11,12]: overloaded volume in the peri-implant areas exhibits a reduction when the implant diameter is increased. In this situation, the contact area between the implant and the neighboring bone increases, and hence the load per unit area transmitted to the peri-implant tissues is decreased, leading to a more favorable stress distribution in the surrounding bone. This is actually the reason why NDIs are associated with higher overloading risks compared to implants of larger diameter.

Regarding the splinting approach, the occurrence of a load sharing effect is unquestionable. In Figure 3, on analyzing the implant supporting the first premolar (P1), both the mean stress and the overloaded volume around the splinted implant in any of the loading scenarios are lower than the values corresponding to the nonsplinted implant analog. This also applies to the implant supporting the first molar (M1). However, to properly quantify the mechanical advantages of the splinting concept, only comparisons between the splinted implant directly loaded (i.e., P1 when loading the first premolar or, alternatively, M1 when loading the first molar) and the nonsplinted implant analog have been made. These two alternative comparisons are appropriate since the peri-implant volumes compared are exactly the same in both the splinted and the nonsplinted stage. Following this logic, the results have shown that 3.0 mm diameter implants splinted by a structure such as the three-unit-bridge analyzed in this study could be considered equivalent to or even more favorable than single 3.5 mm diameter implants in terms of overloading, even if the latter have a larger diameter.



This suggests that the overloading risk associated with NDIs under splinting conditions, specifically when connected by a dental bridge consisting of few dental units, as a FEA study already reported [15], would be comparable to that around RDIs. With this outcome, the capabilities of NDIs, which in FEA studies perform well for the replacement of single upper and lower second premolars, are extended [33]. Accordingly, NDIs splinted by simple dental bridges could be considered in scenarios valid for RDIs but not contemplated for NDIs until now because of their higher resorption risk when operating individually [6].

However, although the three-unit bridge was found to be an interesting approach for compensating the overloading risks of NDIs, the use of this category of implants to support the all-on-four prosthesis proved to involve stress levels even above those found under nonsplinted conditions. Although other FEA studies have shown a similar stress distribution in narrow and regular implants in all-on-four designs, static load was considerably smaller than in our study [34]. As illustrated in Figure 4, the mechanical response of the all-on-four structure is quite sensitive to the area on which the load is applied. Although loading the arch on the first premolar leads to the most favorable situation for the use of NDIs throughout the study, excessive compressive stress around the tilted implant (P2L), especially in cancellous bone, occurs when loading the cantilevered molar. This is in accordance with other studies, that have shown that distal cantilevers in full-arch restorations have a higher overloading risk [35,36]. This overloading of the cortical bone might be especially critical in poorly mineralized cancellous bone [37] or when cortical bone thickness is reduced, as a result of atrophy [38].

As stated by some authors, a class I lever system is generated when a vertical load is applied in the cantilevered region of a prosthesis, and this leverage is one of the main causes for excessive stress concentrations [39,40]. This issue clearly represents a limitation in the compatibility between the splinting approach and NDIs, which seems to largely depend on the type of prosthetic structure involved. However, as a possible solution to significantly reduce the overloading risk around NDIs in this case, the arch could be shortened by removing the cantilevered molars. To reinforce this idea, it should be noted that the value of overloaded volume around P2<sub>L</sub> when loading the second premolar (Figure 4) is lower than that referred to nonsplinted NDIs (Figure 3).

Accordingly, the splinting concept applied to NDIs could be an alternative to the use of larger diameter implants or augmentation procedures when developing prosthetic solutions in which such implants traditionally have been avoided. In fact, the load-sharing effect resulting from the approach is presented as a means of compensating for the higher overloading and resorption risks typically associated with NDIs. However, although this argument seems to be valid for simple structures like the three-unit bridge analyzed, special care should be taken when implants must support cantilever dentures or must be placed in a tilted position, as in the case of the posterior implants in the all-on-four approach. It is worth mentioning that more realistic models overcoming the simplifications assumed in this study should be evaluated, along with more loading conditions and prosthetic solutions, in order to validate the use of splinted NDIs under such circumstances.

## CONCLUSIONS

The structure consisting of a conventional three-unit bridge supported by two implants resulted in a relevant decrease in peri-implant stress in comparison with nonsplinted restorations. The NDIs (diameter 3.0 mm) splinted in this configuration showed an amount of overloaded areas even smaller than in the case of implants belonging to a larger diameter classification (RDIs, diameter 3.5 mm). In contrast, the mechanical benefits resulting from splinting were insufficient to balance the high stress levels when loading the cantilevered molar of an all-on-four superstructure supported by NDIs.

## REFERENCES

1. Schwarz F, Derks J, Monje A, Wang HL. 2018. Peri-implantitis. *J Clin Periodontol.* 45 (Suppl.) :246-66.
2. Palmer RM, Smith BJ, Palmer PJ, Floyd PD. 1997. A prospective study of Astra single tooth implants. *Clin Oral Implants Res.* 8:173-9.
3. Holmgren EP, Seckinger RJ, Kilgren LM, Mante F. 1998. Evaluating Parameters of Osseointegrated Dental Implants Using Finite Element Analysis: A Two-Dimensional Comparative Study Examining the Effects of Implant Diameter, Implant Shape, and Load Direction. *J Oral Implantol.* 24:80–8.
4. Chun HJ, Cheong SY, Han JH, Heo SJ, Chung JP, Rhyu IC, Choi YC, Baik HK, Ku Y, Kim MH. 2002. Evaluation of design parameters of osseointegrated dental implants using finite element analysis. *J Oral Rehabil.* 29:565-74.
5. Klein M, Schiegnitz E, Al-Nawas B. 2014. Systematic Review on Success of Narrow-Diameter Dental Implants. *Int J Oral Maxillofac Implants.* 29(Suppl.):43-54.
6. Galindo-Moreno P, Nilsson P, King P, Becktor J, Speroni S, Schramm A, Maiorana C. 2012. Clinical and radiographic evaluation of early loaded narrow diameter implants: 1-year follow-up. *Clin Oral Implants Res.* 23:609–16.
7. de Souza AB, Sukekava F, Tolentino L, César-Neto JB, Garcez-Filho J, Araújo MG. 2018. Narrow- and regular-diameter implants in the posterior region of the jaws to support single crowns: A 3-year split-mouth randomized clinical trial. *Clin Oral Implants Res.* 29:100-7.
8. Ioannidis A, Gallucci GO, Jung RE, Borzangy S, Hämmerle CH, Benic GI. 2015. Titanium-zirconium narrow-diameter versus titanium regular-diameter implants for anterior and premolar single crowns: 3-year results of a randomized controlled

clinical study. *J Clin Periodontol.* 42:1060-70.

9. Olate S, Lyrio MCN, de Moraes M, Mazzonetto R, Moreira RWF. 2010. Influence of Diameter and Length of Implant on Early Dental Implant Failure. *J Oral Maxillofac Surg.* 68:414–9.
10. Allum SR, Tomlinson RA, Joshi R. 2008. The impact of loads on standard diameter, small diameter and mini implants: A comparative laboratory study. *Clin Oral Implants Res.* 19:553-9.
11. Baggi L, Cappelloni I, Di Girolamo M, Maceri F, Vairo G. 2008. The influence of implant diameter and length on stress distribution of osseointegrated implants related to crestal bone geometry: A three-dimensional finite element analysis. *J Prosthet Dent.* 100:422–31.
12. Ding X, Zhu XH, Liao SH, Zhang XH, Chen H. 2009. Implant-bone interface stress distribution in immediately loaded implants of different diameters: a three-dimensional finite element analysis. *J Prosthodont.* 18:393-402.
13. Guichet DL, Yoshinobu D, Caputo AA. 2002. Effect of splinting and interproximal contact tightness on load transfer by implant restorations. *J Prosthet Dent.* 87:528–35.
14. Jofre J, Hamada T, Nishimura M, Klattenhoff C. 2010. The effect of maximum bite force on marginal bone loss of mini-implants supporting a mandibular overdenture: a randomized controlled trial. *Clin Oral Implants Res.* 21:243–9.
15. Lemos CAA, Verri FR, Santiago Junior JF, de Souza Batista VE, Kemmoku DT, Noritomi PY, et al. 2018. Splinted and nonsplinted crowns with different implant lengths in the posterior maxilla by three-dimensional finite element analysis. *J Healthc Eng.* 2018:3163096.
16. Katranji A, Misch K, Wang H-L. 2007. Cortical Bone Thickness in Dentate and Edentulous Human Cadavers. *J Periodontol.* 78:874–8.

17. Maló P, de Araújo Nobre M, Lopes A, Francischone C, Rigolizzo M. 2012. “All-on-4” immediate-function concept for completely edentulous maxillae: a clinical report on the medium (3 years) and long-term (5 years) outcomes. *Clin Implant Dent Relat Res.* 14(Suppl.):139-50.
18. Van Oosterwyck H, Duyck J, Sloten J Vander, Van Der Perre G, De Cooman M, Lievens S, Puers R, Naert I. 1998. The influence of bone mechanical properties and implant fixation upon bone loading around oral implants. *Clin Oral Implants Res.* 9:407-18.
19. Chun H-J, Park D-N, Han C-H, Heo S-J, Heo M-S, Koak J-Y. 2005. Stress distributions in maxillary bone surrounding overdenture implants with different overdenture attachments. *J Oral Rehabil.* 32:193–205.
20. Colling EW. 1984. The physical metallurgy of titanium alloys. Metals Park: OH: American Society for Metals.
21. Craig RG. 1989. Restorative dental materials. St. Louis: Mosby.
22. Ferrario VF, Sforza C, Serrao G, Dellavia C, Tartaglia GM. 2004. Single tooth bite forces in healthy young adults. *J Oral Rehabil.* 31:18–22.
23. Özdemir Doğan D, Polat NT, Polat S, Şeker E, Gül EB. 2014. Evaluation of “All-on-Four” concept and alternative designs with 3D finite element analysis method. *Clin Implant Dent Relat Res.* 16:501-10.
24. Koolstra JH, van Eijden TMGJ, Weijs WA, Naeije M. 1988. A three-dimensional mathematical model of the human masticatory system predicting maximum possible bite forces. *J Biomech.* 21:563-76.
25. Borie E, Orsi I, Noritomi P, Kemmoku D. 2016. Three-Dimensional Finite Element Analysis of the Biomechanical Behaviors of Implants with Different Connections, Lengths, and Diameters Placed in the Maxillary Anterior Region. *Int J Oral*

Maxillofac Implants. 31:101–10.

26. Martin RB, Burr DB, Sharkey NA, Fyhrie DP. 1998. Skeletal tissue mechanics. New York: Springer.
27. Ashrafi M, Ghaliachi F, Mirzakouchaki B, Arruga A, Doblare M. 2019. Finite element comparison of the effect of absorbers' design in the surrounding bone of dental implants. *Int J Numer Method Biomed Eng.* 5:e3270.
28. Udomsawat C, Rungsiyakull P, Rungsiyakull C, Khongkhunthian P. 2018. Comparative study of stress characteristics in surrounding bone during insertion of dental implants of three different thread designs: A three-dimensional dynamic finite element study. *Clin Exp Dent Res.* 5:26-37.
29. Cali M, Zanetti EM, Oliveri SM, Asero R, Ciaramella S, Martorelli M, Bignardi C. 2018. Influence of thread shape and inclination on the biomechanical behaviour of plateau implant systems. *Dent Mater.* 34:460-9.
30. Maminskas J, Puisys A, Kuoppala R, Raustia A, Juodzbals G. 2016. The prosthetic influence and biomechanics on peri-implant strain: a systematic literature review of finite element studies. *J Oral Maxillofac Res.* 7:e4.
31. Trivedi, S. 2014. Finite element analysis: A boon to dentistry. *Journal of Oral Biology and Craniofacial Research.* 4:200-03
32. Duan Y, Gonzalez JA, Kulkarni PA, Nagy WW, Griggs JA. 2018. Fatigue lifetime prediction of a reduced-diameter dental implant system: Numerical and experimental study. *Dent Mater.* 34:1299-309.
33. Cinel S, Celik E, Sagirkaya E, Sahin O. 2018. Experimental evaluation of stress distribution with narrow diameter implants: A finite element analysis. *J Prosthet Dent.* 119:417-25.
34. Moreira de Melo EJ Jr, Francischone CE. 2019. Three-dimensional finite element

analysis of two angled narrow-diameter implant designs for an all-on-4 prosthesis. *J Prosthet Dent*.30607-9.

35. Ozan O, Kurtulmus-Yilmaz S. 2018. Biomechanical comparison of different implant inclinations and cantilever lengths in All-on-4 treatment concept by three-dimensional finite element analysis. *Int J Oral Maxillofac Implants*.33:64-71.
36. Cenkoglu BG, Balcioglu NB, Ozdemir T, Mijiritsky E. 2019. The effect of the length and distribution of implants for fixed prosthetic reconstructions in the atrophic posterior maxilla: A finite element analysis. *Materials (Basel)*.11;12.
37. Azcarate-Velázquez F, Castillo-Oyagüe R, Oliveros-López LG, Torres-Lagares D, Martínez-González ÁJ, Pérez-Velasco A, et al. 2019. Influence of bone quality on the mechanical interaction between implant and bone: A finite element analysis. *J Dent*.88:103161.
38. Ueda N, Takayama Y, Yokoyama A. 2017. Minimization of dental implant diameter and length according to bone quality determined by finite element analysis and optimized calculation. *J Prosthodont Res*.61:324-32.
39. Krekmanov L, Kahn M, Rangert B, Lindström H. 2000. Tilting of posterior mandibular and maxillary implants for improved prosthesis support. *Int J Oral Maxillofac Implant*. 15:405–14.
40. Aparicio C, Perales P, Rangert B. 2001. Tilted implants as an alternative to maxillary sinus grafting: A clinical, radiologic, and periotest study. *Clin Implant Dent Relat Res*. 3:39-49.



## LEGENDS

Table 1: Material properties.

Figure 1: 3D CAD models of the three prosthetic scenarios analyzed: a) single-implant restoration; b) three-unit bridge; c) all-on-four rehabilitation. An example of a peri-implant VOI is also shown: in red, overloaded cancellous bone; in dark blue, overloaded cortical bone.

Figure 2: In rows: minimum principal stress and maximum principal stress generated when loading the first premolar in the single-implant restoration and the three-unit bridge. In columns: different implant diameters ( $\varnothing$  3.0 mm,  $\varnothing$  3.5 mm and  $\varnothing$  4.3 mm). The images of the three-unit bridge rehabilitation include the plane containing the implant at the first premolar site (P1) and the plane containing the implant at the first molar site (M1).

Figure 3: In rows: mean maximum principal stress and mean minimum principal stress ( $\langle \sigma_{p\ max} \rangle$  and  $\langle \sigma_{p\ min} \rangle$ , represented with bars and stated on the left axis) and overloaded volume ( $OV_T$ ,  $OV_C$  and  $OV$ , represented with +, - and  $\blacklozenge$ , respectively, and stated on the right axis) in cancellous and cortical bone within the VOIs analyzed.  $OV_T$ ,  $OV_C$  and  $OV$  denote overloaded volume under tension, overloaded volume under compression and total overloaded volume ( $OV = OV_T + OV_C$ ), respectively. P1, P2 and M1 denote the data corresponding to the VOIs around the first premolar, second premolar and first molar,

respectively. In columns: different loading conditions; the tooth loaded is shown in red color.

Figure 4: Minimum principal stress and maximum principal stress (in rows) of the model corresponding to the all-on-four rehabilitation with 3 mm diameter implants for the three loading conditions analyzed (in columns). Each of the 6 images depict two different planes: a frontal plane containing the anterior **left and right** implants ( $I_L$  and  $I_R$ ), and a plane containing the axes of the tilted implant closest to the loading area ( $P2_L$ ) and its abutment-screw. The last row includes the overloaded volume in the peri-implant VOI around  **$P2_{RL}$**  when considering different implant diameters ( $\varnothing$  3.0 mm,  $\varnothing$  3.5 mm and  $\varnothing$  4.3 mm).

Formatted: Highlight

Formatted: Highlight

TABLE 1

Component and material	Elastic Modulus (GPa)	Poisson Ratio
Cortical bone [17]	13.7	0.3
Cancellous bone [18]	0.5	0.3
Implants and abutments: Ti-6Al-4V [19]	110	0.35
Superstructures: Cr-Co alloy [20]	218	0.33

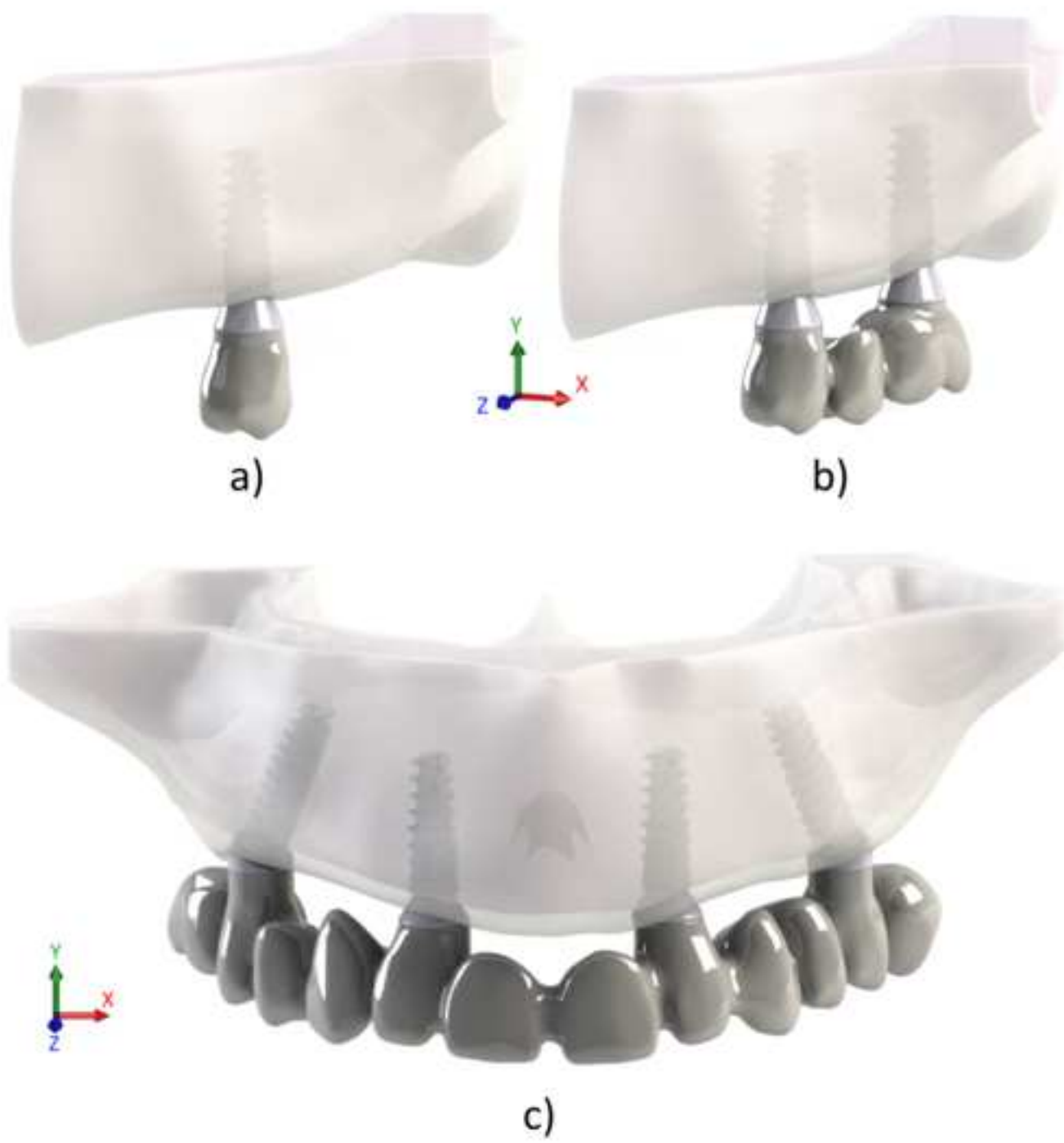


Figure 2

[Click here to access/download;Figure;Figura 2.png](#)

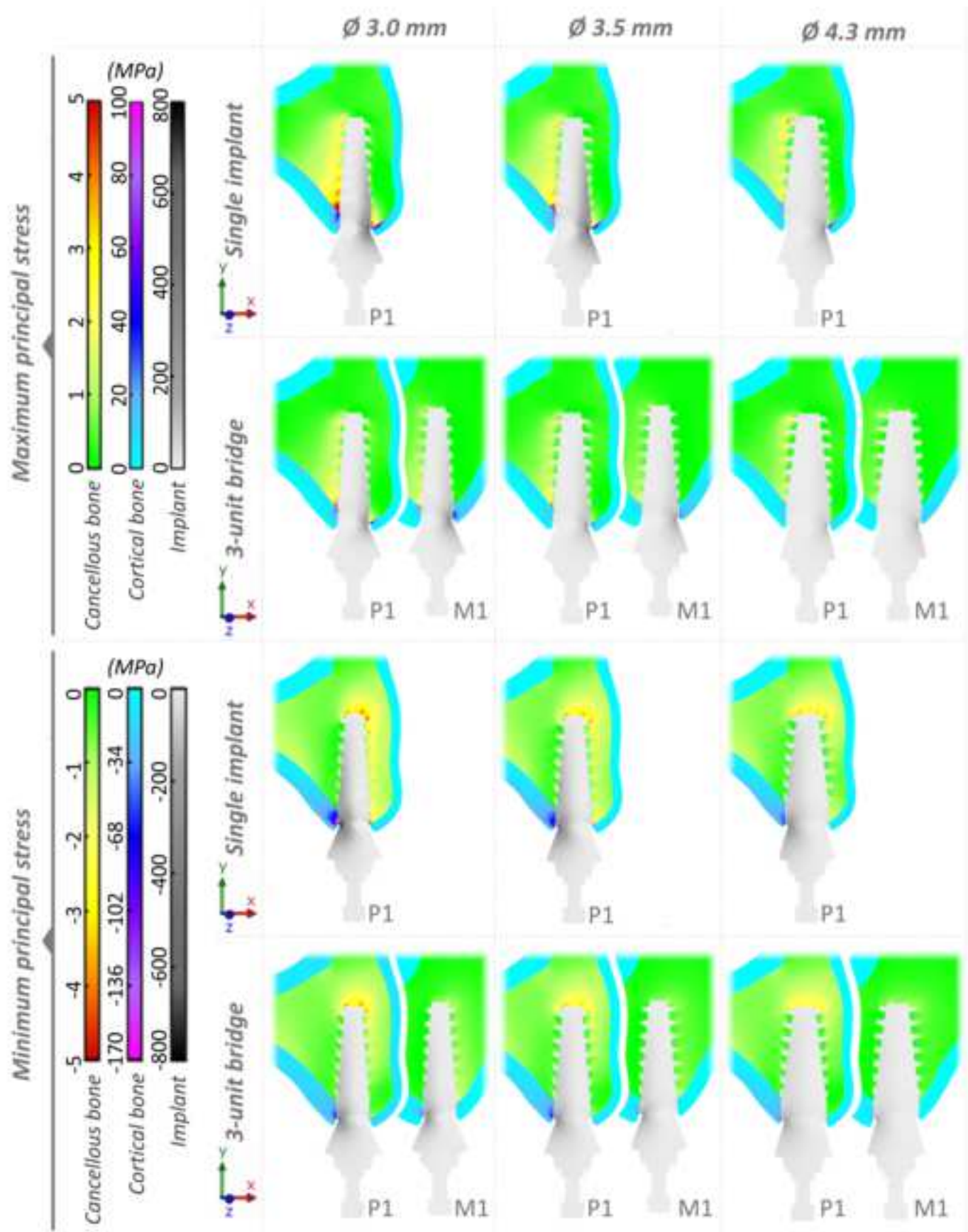


Figure 3

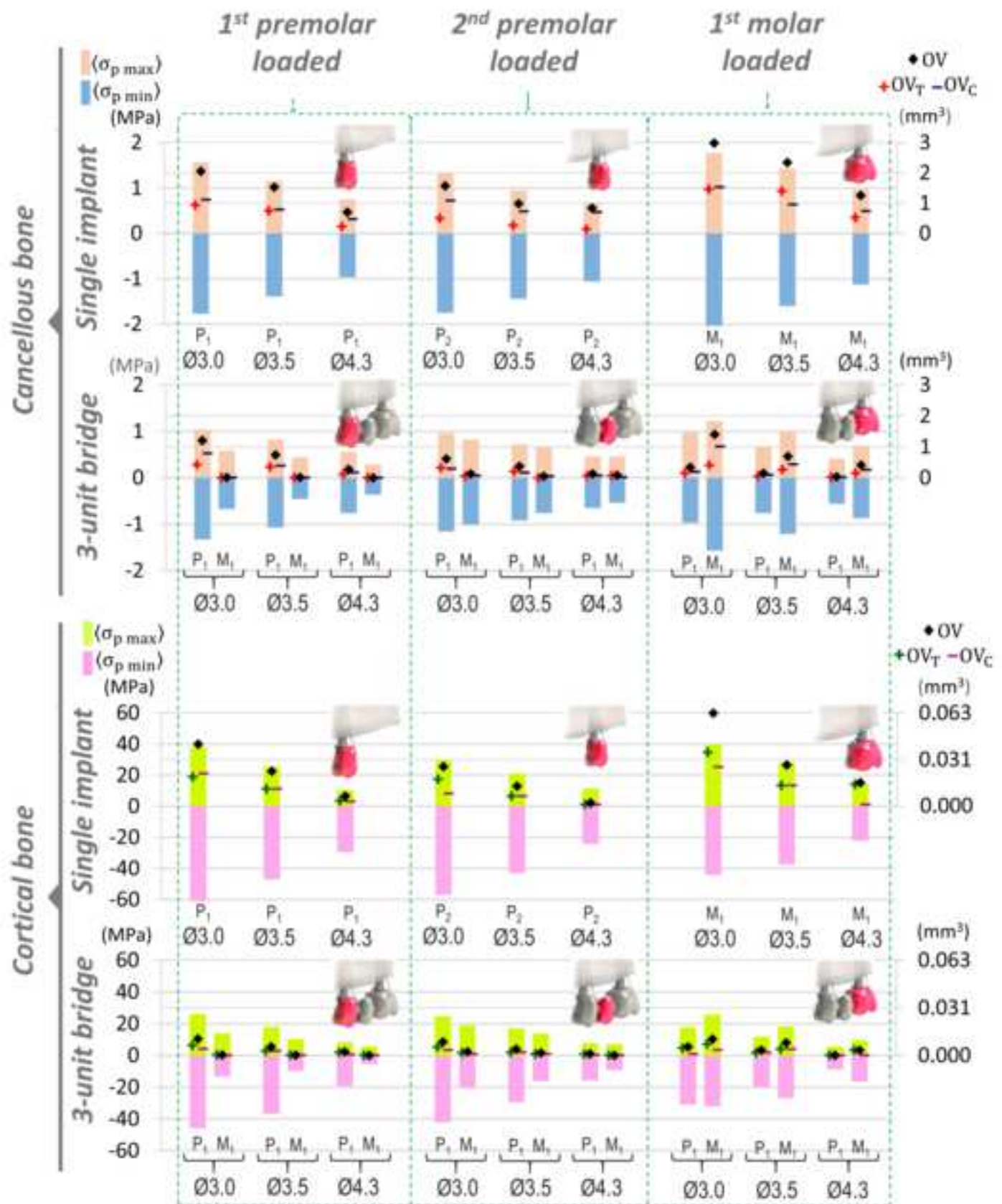
[Click here to access/download;Figure;Figure 3.png](#)



Figure 4

[Click here to access/download;Figure;Figure 4.png](#)

